In vivo analysis of the contribution of proprotein convertases to the processing of FGF23

Running title: Proprotein convertases in the regulation of FGF23

Omar Al Rifai[1,2], Delia Susan-Resiga[3], Rachid Essalmani[3], John W.M. Creemers[4], Nabil G. Seidah[3] and Mathieu Ferron[1,2,5,6]#

[1] Unité de recherche en physiologie moléculaire, Institut de Recherches Cliniques de Montréal, Montréal, Québec H2W 1R7, Canada
[2] Programme de biologie moléculaire, Université de Montréal, Québec H3T 3J7, Canada
[3] Unité de recherche en biochimie neuroendocrinienne, Institut de Recherches Cliniques de Montréal, Montréal, Québec H2W 1R7, Canada
[4] Department of Human Genetics, KU Leuven, Herestraat 49, B-3000 Leuven, Belgium
[5] Département de Médecine, Université de Montréal, Québec H3T 3J7, Canada
[6] Division of Experimental Medicine, McGill University, Montréal, Québec H3A 1A3, Canada

Omar.alrifai@ircm.qc.ca; Delia.Susan-Resiga@ircm.qc.ca; Rachid.Essalmani@ircm.qc.ca; john.creemers@kuleuven.be; Nabil.Seidah@ircm.qc.ca; mathieu.ferron@ircm.qc.ca

Correspondence to:

Mathieu Ferron, PhD
Institut de Recherches Cliniques de Montréal
110 Ave. des Pins O.
Montréal, QC,
H2W 1R7, Canada
Phone: 514-987-5754
Fax: 514-987-5649
Email: mathieu.ferron@ircm.qc.ca

Author contributions: MF, DSR and OAR conceived and planned the experiments. OAR and DSR carried out the experiments. OAR and MF analyzed the data. RE, JWMC and NGS provided critical mouse lines. OAR and MF wrote the manuscript with input from all authors.

Keywords

FGF23, endoproteolysis, proprotein convertases, Furin, PC5, PACE4, phosphate

ABSTRACT

Fibroblast growth factor 23 (FGF23) is a hormone secreted from fully differentiated osteoblasts and osteocytes that inhibits phosphate reabsorption by kidney proximal tubules. The full-length (i.e., intact) protein mediates FGF23 endocrine functions, while endoproteolytic cleavage at a consensus cleavage sequence for the proprotein convertases (PCs) inactivates FGF23. Two PCs, furin and PC5, were shown to cleave FGF23 *in vitro* at $RHTR_{179}\downarrow$, but whether they are fulfilling this function in vivo is currently unknown. To address this question we used here mice lacking either or both furin and PC5 in cell-specific manners and mice lacking the paired basic amino acid-cleaving enzyme 4 (PACE4) in all cells. Our analysis shows that furin inactivation in osteoblasts and osteocytes results in a 25% increase in circulating intact FGF23, without any significant impact on serum phosphate levels, whether mice are maintained on a normal or a low phosphate diet. Under conditions of iron deficiency, FGF23 is normally processed in control mice, but its processing is impaired in mice lacking furin in osteoblasts and osteocytes. In contrast, FGF23 is normally cleaved following erythropoietin or IL-1β injections in mice lacking furin or both furin and PC5, and in PACE4-deficient mice. Altogether, these studies suggest that furin is only partially responsible for FGF23 cleavage under certain conditions *in vivo*. The processing of FGF23 may therefore involve the redundant action of multiple PCs or of other peptidases in osteoblasts, osteocytes and hematopoietic cells.

58 **INTRODUCTION**

59 Fibroblast growth factor 23 (FGF23) is a bone-derived hormone (i.e., osteokine)
60 secreted by fully differentiated osteoblasts and osteocytes. FGF23 plays a fundamental
61 role in phosphate and vitamin D metabolism through a direct action on the kidney [1,2]. In
62 this tissue, its signaling is mediated through interaction with the FGF receptor 1
63 (FGFR1) and its co-receptor α-klotho [3]. FGF23 signaling through FGFR1/α-klotho in the
64 kidney proximal tubule suppresses the expression of *Slc34a1* and *Slc34a3*, the genes
65 encoding for the sodium phosphate co-transporters NaPi2A and NaPi2C, thereby
66 increasing urinary phosphate excretion and decreasing serum phosphate levels. In
67 addition, FGF23 reduces the 1,25-dihydroxyvitamin D_3 (calcitriol) level by decreasing
68 expression of *Cyp27b1* which encodes the 25-hydroxyvitamin D-1 alpha hydroxylase
69 and increasing expression of *Cyp24a1* which encodes the 1,25-dihydroxyvitamin D_3 24-
70 hydroxylase [4-7]. These endocrine functions are mediated through full-length or intact
71 FGF23 (amino acids [aa] 25-251). Endoproteolytic cleavage of FGF23 at the basic motif
72 **R**$_{176}$HT**R**$_{179}$↓SA, a consensus cleavage site for proprotein convertases (PCs), releases
73 N-terminal (aa 25-179) and C-terminal (aa 180-251) fragments and inactivates FGF23.
74

75 Circulating intact FGF23 levels are tightly regulated in part through various post-
76 translational modifications of amino acids surrounding the PC cleavage site. For
77 instance, the *O*-glycosylation of threonine 178 (T_{178}) by the *N*-
78 acetylgalactosaminyltransferase 3 (GalNAc-T3) inhibits FGF23 processing [8-10]. FGF23
79 *O*-glycosylation is in turn reduced when the serine 180 (S_{180}) is phosphorylated by
80 Fam20c, a kinase residing in the Golgi [11]. Impaired FGF23 glycosylation caused either

81 by a defective GalNAc-T3 or mutation in FGF23 glycosylation sites, results in an
82 increase in FGF23 processing and subsequent decrease in circulating intact FGF23
83 levels. These molecular defects lead to familial tumoral calcinosis (FTC), a human
84 disease characterized by hyperphosphatemia and heterotopic calcification [8-10]. On the
85 other hand, mutations in the FGF23 cleavage site and in the X-linked phosphate-
86 regulating neutral endopeptidase (PHEX) respectively cause autosomal dominant
87 hypophosphatemic rickets (ADHR) and X-linked hypophosphatemic rickets (XLH) that
88 are characterized by hypophosphatemia and osteomalacia due to the increased level of
89 active intact FGF23 [12,13].
90
91 Iron deficiency, erythropoietin treatment or interleukin-1 beta (IL-1β) stimulate FGF23
92 production by osteocytes and bone marrow hematopoietic cells [14-19]. However, this
93 increase in FGF23 production only results in the accumulation of intact FGF23 levels
94 and hypophosphatemia in ADHR patients or in mice with an ADHR-like mutation in
95 *Fgf23*. In wildtype animals or healthy subjects, the same stimuli result in increased
96 circulating levels of cleaved FGF23, revealing the importance of endoproteolysis by PC
97 for the regulation of this hormone.
98
99 The proprotein convertases furin and PC5 can cleave FGF23 *in vitro* [20], and *FURIN*
100 inactivation in the human osteosarcomas U2-OS cell line impaired the cleavage of
101 ectopically expressed human FGF23 [11]. Nevertheless, the identity of the enzyme(s)
102 responsible for FGF23 endoproteolysis *in vivo* remains undetermined. In the present
103 study we assessed whether furin and PC5 cleave FGF23 in vivo and affect phosphate

104 metabolism. We showed that unlike what is the case in vitro, furin inactivation in the
105 osteoblastic lineage results only in a modest increase in intact FGF23 under normal or
106 low phosphate diet, but impairs FGF23 cleavage in conditions of iron deficiency. We
107 also show that furin, PC5 and PACE4, another PC expressed in osteoblasts, which all
108 can cleave FGF23 *in vitro*, failed to do so *in vivo* following treatment with erythropoietin
109 or IL-1β. Together, our data suggest that furin, PC5 and PACE4 may not be the main
110 PCs cleaving FGF23 *in vivo*.

111 **RESULTS**

112

113 **In vivo inactivation of Furin in osteoblasts and osteocytes partially impairs FGF23**
114 **cleavage, but decreases phosphate excretion**

115 To investigate the role of furin in the regulation of FGF23 processing *in vivo*, we
116 generated mice in which the *Furin* gene was specifically inactivated in osteoblasts and
117 osteocytes (i.e., *Furin*^{osb}*-/-*) by breeding *Furin*$^{fl/fl}$ mice with hOCN-Cre transgenic animals
118 which express the Cre recombinase under the control of human osteocalcin promoter [21].
119 We previously reported that the *Furin* gene was efficiently and specifically inactivated in
120 osteoblasts and bones in these mice [22]. Although the precursor of osteocalcin, another
121 bone-derived hormone involved in the control of glucose homeostasis, is not processed
122 in *Furin*^{osb}*-/-* mice, the same animals do not develop glucose intolerance before 9
123 months of age [22]. Thus, to avoid a potential confounding effect of hyperglycemia on
124 FGF23 and phosphate metabolism, all the following experiments were performed on
125 mice aged between 3 and 6 months. When fed a normal chow diet containing ~0.7%
126 inorganic phosphate (Pi), 4-month-old *Furin*^{osb}*-/-* female mice displayed a significant
127 25% rise in circulating intact FGF23 (Figure 1A). This rise was however more moderate
128 than expected in view of in vitro-based studies [11] and did not significantly alter the
129 expression of *Slc34a1*, *Slc34a3*, *Cyp27b1* or *Cyp24a1* (Figure 1B). Accordingly,
130 *Furin*^{osb}*-/-* mice maintained normal serum phosphate levels and bone histology did not
131 reveal presence of osteomalacia (Figure 1C and D).

132

133 Serum phosphate level is a potent regulator of FGF23 and in mice fed a low-phosphate
134 synthetic diet the circulating intact FGF23 levels are reduced, while those of the
135 processed fraction are increased, presumably due to the action of one or several PCs
136 [23-25]. We therefore next assessed if severe hypophosphatemia would be induced in
137 *Furin*^{osb}*-/-* mice by reducing their phosphate intake. We found that feeding control and
138 *Furin*^{osb}*-/-* mice a low-phosphate diet (0.02% Pi) for one week did not affect body weight

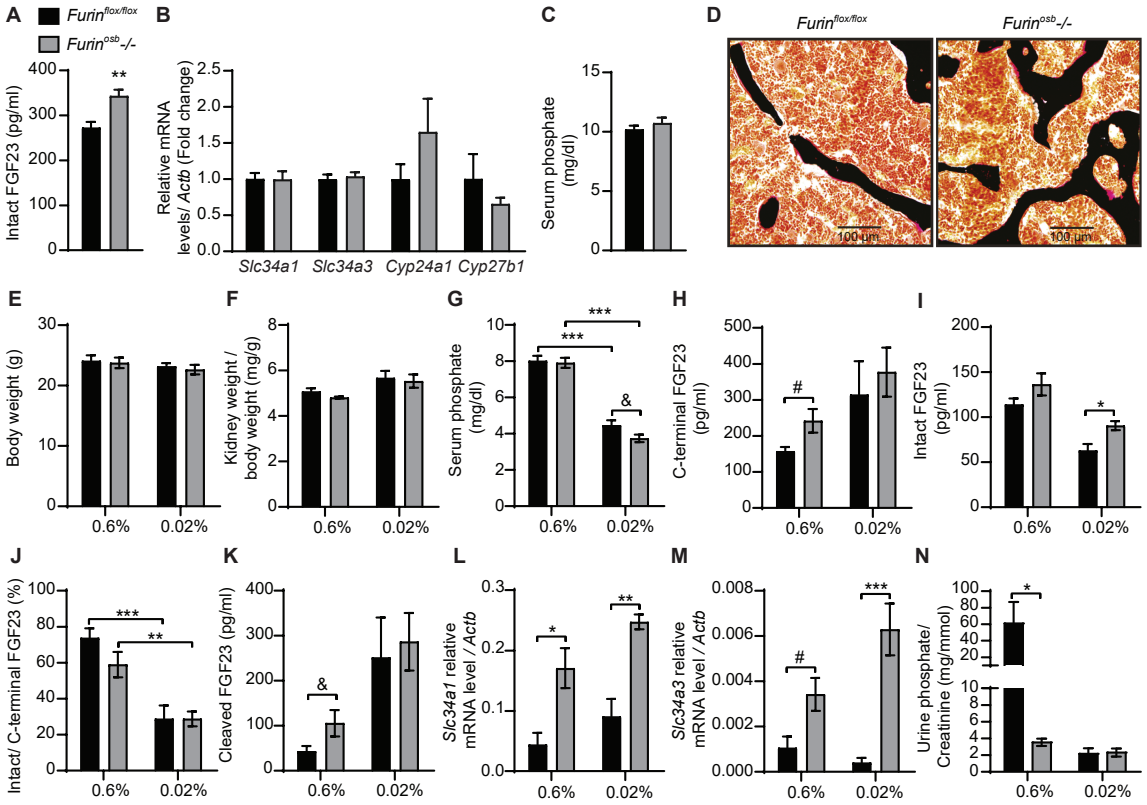

139 **Figure 1: Increased FGF23 level and reduced phosphate excretion in *Furin*^{osb}*-/-* mice.** FGF23 and
140 phosphate levels in in 4-month-old *Furin*$^{flox/flox}$ (n=6) and *Furin*^{osb}*-/-* (n=6) mice fed on normal chow diet **(A-**
141 **D)**. Intact FGF23 levels in plasma **(A)**. FGF23 target genes expression in kidney **(B)**. Serum phosphate
142 level **(C)**. Von Kossa / van Gieson staining on vertebrae sections **(D)**. FGF23 and phosphate parameters
143 in 6-months-old *Furin*$^{flox/flox}$ (n=6) and *Furin*^{osb}*-/-* (n=6-7) mice fed a normal phosphate diet (0.6%) or a low
144 phosphate diet (0.02%) for one week **(E-N)**. Body weight **(E)**. Kidney weight normalize to body weight **(F)**.
145 Serum phosphate levels **(G)**. Plasma level of C-terminal FGF23 **(H)**, intact FGF23 **(I)**, percentage (%) of
146 intact over C-terminal FGF23 **(J)** and cleaved FGF23 levels **(K)** calculated as (C-terminal FGF23) - (intact
147 FGF23). Expression level in kidney of the sodium phosphate cotransporter *Slc34a1* **(L)** and *Slc34a3* **(M).**
148 **(N)** Urine phosphate measurements normalized to creatinine. Results represent the mean ± SEM. **P* <
149 0.05, ***P* < 0.01, and ****P* < 0.001, by 2-way ANOVA with Bonferroni's multiple comparisons test or by
150 Student's t-test (A, C, G, H, K, and M) #: *P*<0.05; # #: *P*<0.01, # # #: *P*<0.001 &: 0.05<*P*<0.1.
151

152 or kidney weight (Figure 1E and F), but significantly decreased serum phosphate level
153 (Figure 1G). Under the same conditions, *Furin*^{osb}*-/-* mice tend to have a lower serum
154 phosphate level compared to control mice, although this did not reach statistical
155 significance. *Furin*^{osb}*-/-* mice on normal diet had >25% increase in intact and C-terminal
156 (total) FGF23, while maintaining normal intact/C-terminal FGF23 ratio compared to
157 control littermates (Figure 1H-J). Under low phosphate diet circulating intact FGF23 was
158 reduced in control mice, but remains significantly higher in *Furin*^{osb}*-/-* mice (Figure 1I).
159 However, the ratio of intact over C-terminal FGF23 was decreased in both control and
160 *Furin*^{osb}*-/-* mice under low phosphate diet (Figure 1J). Moreover, the amount of
161 circulating cleaved FGF23 (i.e., C-terminal FGF23 minus intact FGF23) was increased
162 on low phosphate diet regardless of the genotype, suggesting efficient cleavage of
163 FGF23 even in absence of furin (Figure 1K). These results suggest that in conditions of
164 normal or low phosphate intake, processing of FGF23 still occurs in absence of furin in
165 osteoblasts and osteocytes.
166
167 Surprisingly, when fed synthetic normal or low phosphate diets, *Furin*^{osb}*-/-* mice
168 displayed an increased expression in the kidney of the sodium phosphate transporter
169 genes *Slc34a1* and *Slc34a3* compared to control mice, regardless of the level of
170 phosphate in the diet (Figure 1L and M). In addition, *Furin*^{osb}*-/-* mice fed the normal
171 phosphate diet showed a decrease in urinary phosphate compared to control littermate
172 (Figure 1N). Challenging the mice for one week on the low phosphate diet reduced
173 urinary phosphate in control mice as expected, but not in *Furin*^{osb}*-/-* mice, as these mice
174 maintained the low urinary phosphate observed on normal phosphate diet (Figure 1N).

175 Together these results show that unlike what was observed in vitro, in both
176 physiological conditions or during decreased phosphate intake, inactivation of *Furin* in
177 the osteoblast lineage has only a modest impact on FGF23 processing. They also
178 suggest that furin may influence phosphate excretion through FGF23-independent
179 mechanisms.
180

181 **Furin contributes to FGF23 processing during iron deficiency**

182 It was previously reported that mice carrying an ADHR mutation (R176Q, i.e., loss of P4
183 Arg in the motif **R**$_{176}$HT**R**$_{179}$↓SA) in the *Fgf23* gene did not develop hypophosphatemia
184 unless they were fed a low-iron diet [15]. In view of these observations, we induced iron-
185 deficiency in control and *Furin*^{osb}*-/-* mice by feeding them a low-iron diet in combination
186 with repeated tail bleedings (i.e., ~70 μl every other week) for 14 weeks, before
187 assessing the impact on FGF23 and phosphate metabolism. Control and *Furin*^{osb}*-/-*
188 mice fed this diet grew normally (Figure 2A), but both developed iron deficiency as
189 reflected by the decrease in hepcidin (*Hamp*) expression and the increase in transferrin
190 receptor (*Tfrc*) expression in liver (Figure 2B-C). As previously shown [15], iron deficient
191 control and *Furin*^{osb}*-/-* mice displayed an increase in *Fgf23* gene expression in bone
192 (Figure 2D). However, iron-deficiency resulted in increased in circulating C-terminal
193 FGF23 only in control mice, although both genotypes showed an increase in circulating
194 intact FGF23 (Figure 2E-F). These results indicate that FGF23 processing appears to
195 be severely impaired in *Furin*^{osb}*-/-* mice under conditions of iron deficiency as these
196 mice maintained in the circulation a 1:1 ratio (i.e., 100%) of intact over C-terminal
197 FGF23 and very low level of cleaved FGF23 (Figure 2G-H). Despite this near complete

198 inhibition in FGF23 processing, iron deficient *Furin*^{osb}*-/-* mice displayed a paradoxical
199 increase in serum phosphate level compared to the control littermates fed the same diet
200 (Figure 2I). Altogether these results suggest that furin maybe the main PC responsible
201 of FGF23 processing under iron deficiency.

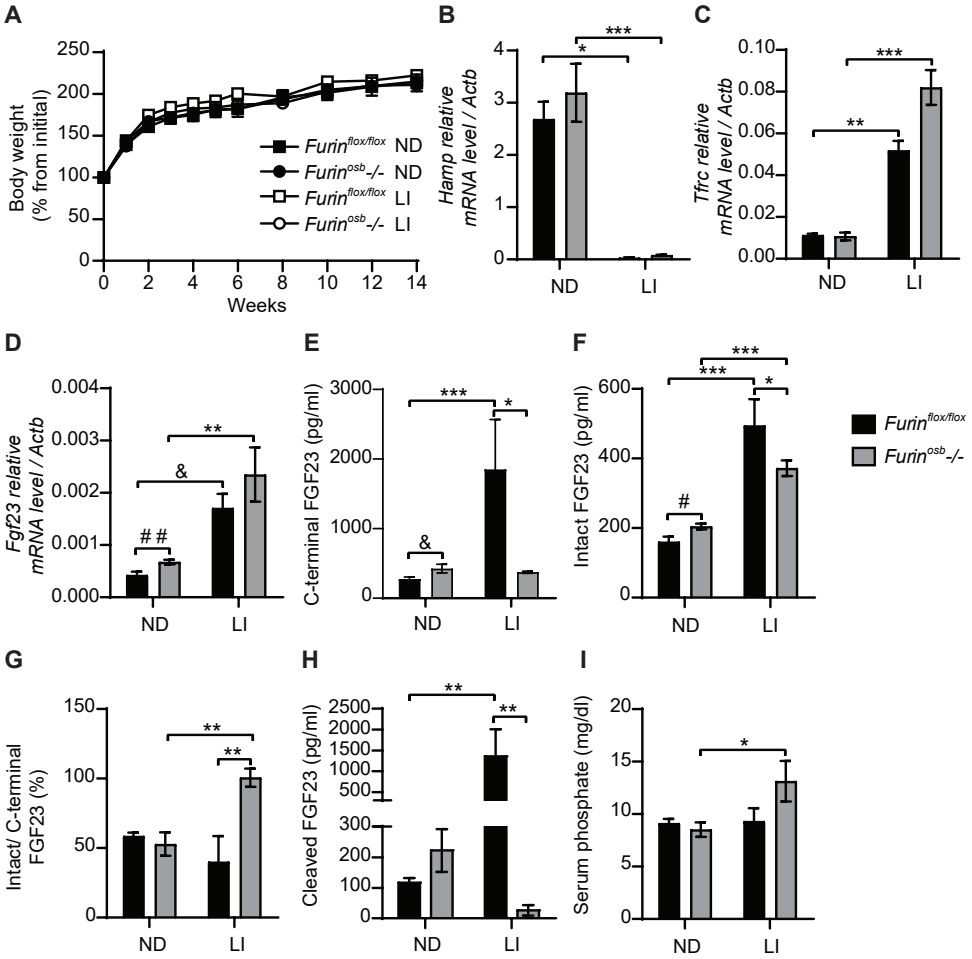

202 **Figure 2: Impaired FGF23 processing in *Furin*^{osb}*-/-* mice following iron restriction.** *Furin*$^{flox/flox}$ (n=3-5)
203 and *Furin*^{osb}*-/-* (n=7-8) 21-day-old mice were fed normal chow diet (ND) or a low iron diet (LI) for 14
204 weeks. **(A)** Body weight growth curve presented as percentage of initial body weight. **(B-C)** Expression of
205 iron-regulated genes in liver. Hepcidin (*Hamp*) expression **(B)**. Transferrin receptor (*Tfrc*) expression **(C).**
206 **(D)** *Fgf23* expression in long bone. **(E-H**) Plasma level of C-terminal FGF23 **(E)**, intact FGF23 **(F)**,
207 percentage (%) of intact over C-terminal FGF23 **(G)** and cleaved FGF23 levels **(H)**, calculated as (C-
208 terminal FGF23) - (intact FGF23). **(I)** Serum phosphate levels. Results represent the mean ± SEM. **P* <
209 0.05, ***P* < 0.01, and ****P* < 0.001, by 2-way ANOVA with Bonferroni's multiple comparisons test or by
210 Student's t-test (D and E) #: *P*<0.05; # #: *P*<0.01, # # #: *P*<0.001 &: 0.05<*P*<0.1.
211

212

213 **Furin does not process FGF23 in osteoblasts and osteocytes following rhEPO**
214 **and IL-1β injections**

215 Erythropoietin and interleukin 1 beta (IL-1β), which are increased in condition of anemia
216 and inflammation respectively, are two potent inducers of *Fgf23* at the transcriptional
217 level [16-19,26,27]. In wild type mice, the majority of circulating FGF23 (i.e., >80%) is cleaved
218 following injection of either recombinant human erythropoietin (rhEPO) or IL-1β [16,17,19],
219 suggesting the action of one or several PCs. Hence, we tested if furin contributes to
220 FGF23 processing after a single injection of rhEPO or IL-1β. We first confirmed that two
221 relatively low doses of rhEPO (i.e., 300U/kg and 3000U/kg) were sufficient to induce in
222 bones and bone marrow of wild type C57BL/6J mice the expression of two known EPO
223 target genes, erythropoietin receptor (*Epor*) and erythroferrone (*Erfe*) (Figure 3A-D).
224 These two doses also robustly induced *Fgf23* expression in both tissues (Figure 3E-F).
225 We next assessed the effect of the same dose of rhEPO in control and *Furin*^{osb}*-/-* mice
226 on the various circulating forms of FGF23. Circulating levels of total (i.e., C-terminal)
227 FGF23 were increased dose-dependently following rhEPO injections, while circulating
228 intact FGF23 levels were only modestly changed in both control and *Furin*^{osb}*-/-* mice
229 (Figure 3G-H). The ratio of intact over C-terminal FGF23 level was robustly reduced by
230 the same treatment (Figure 3I) and cleaved FGF23 was increased more than 10-fold by
231 rhEPO in both control and *Furin*^{osb}*-/-* mice (Figure 3J), suggesting that following rhEPO,
232 FGF23 is normally processed even in absence of furin in osteoblasts and osteocytes.
233

234 In separate experiments, control and *Furin*^{osb}*-/-* mice were administered a single dose of

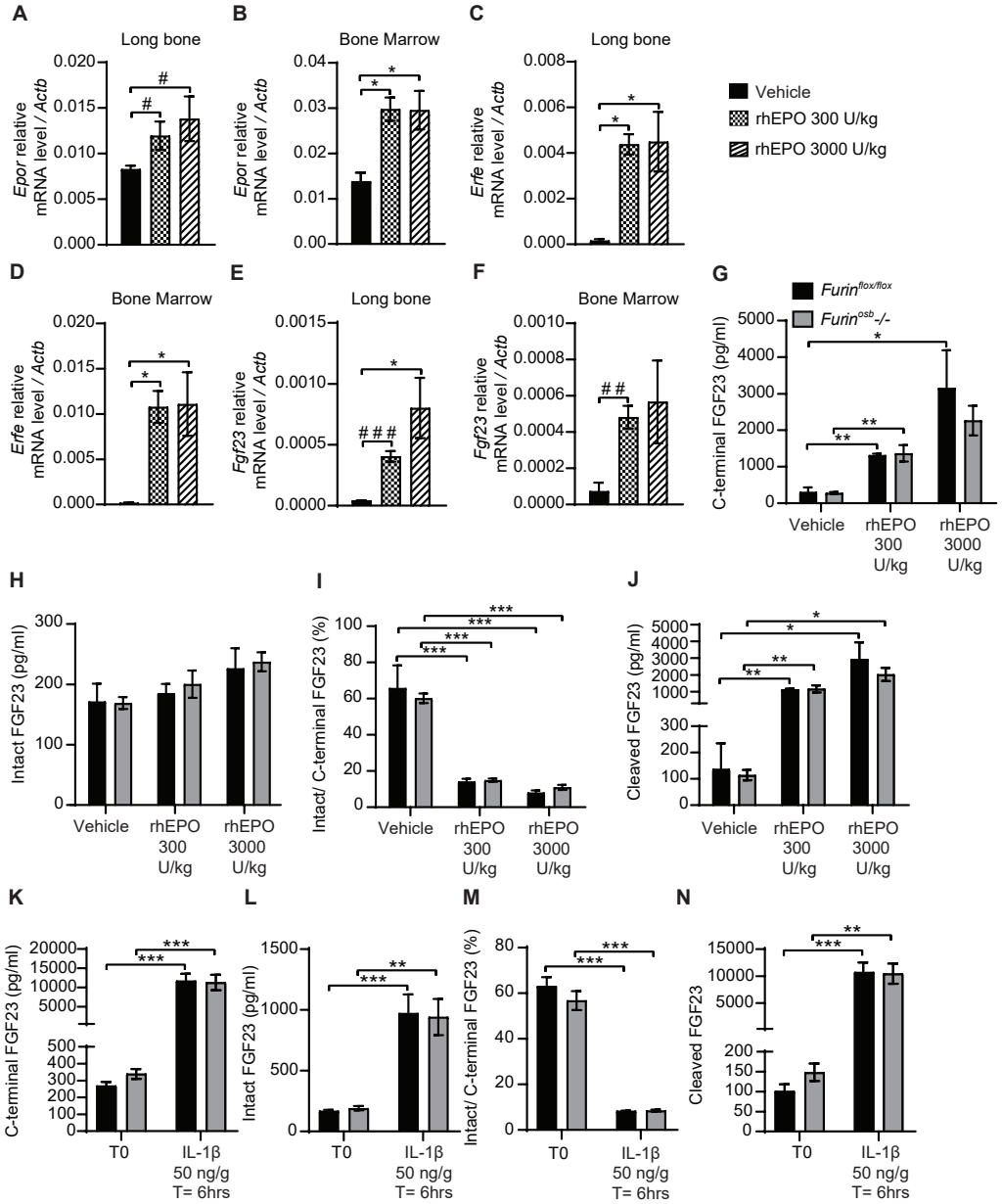

Figure 3: FGF23 is normally processed following erythropoietin and IL-1β injection in *Furin*^{osb}-/- mice. Genes expression in long bone **(A, B and E)** and bone marrow **(C, D and F)** of 2-month-old C57BL/6J mice 6 hours following the injection of vehicle (n=4), 300 U/kg (n=4) or 3000 U/kg (n=4) of recombinant human erythropoietin (rhEPO). Erythropoietin receptor (*Epor*) **(A and C)**, erythroferrone (*Erfe*) **(B and D)** and FGF23 (*Fgf23*) **(C and F)**. **(G-J)** Plasma FGF23 measurements in 4-month-old *Furin*$^{flox/flox}$ (n=3) and *Furin*^{osb}-/- (n=3) mice 6 hours following the injection of vehicle, 300 U/kg or 3000 U/kg of rhEPO. C-terminal FGF23 **(G)**, intact FGF23 **(H),** percentage (%) of intact over C-terminal FGF23 **(I)** and cleaved FGF23 levels **(J)**, calculated as (C-terminal FGF23) - (intact FGF23). **(K-N)** Plasma FGF23 measurements in 4-month-old *Furin*$^{flox/flox}$ (n=4) and *Furin*^{osb}-/- (n=4) mice before (T0) and 6 hours following the injection of 50 ng/g IL-1β (T=6hrs). C-terminal FGF23 **(K)**, intact FGF23 **(L),** percentage (%) of intact over C-terminal FGF23 **(M)** and cleaved FGF23 levels **(N)**. Results represent the mean ± SEM. *P < 0.05, **P < 0.01, and ***P < 0.001, by 1-way ANOVA **(A-F)** or 2-way ANOVA **(G-N)** with Bonferroni's multiple comparisons test, or by Student's t-test **(A and E)** #: P<0.05; # #: P<0.01, # # #: P<0.001 &: 0.05<P<0.1.

249 IL-1β (50ng/g), that induces *Fgf23* expression in bone and raises circulating total and
250 cleaved FGF23 levels [16]. Six hours after the injection of IL-1β, the circulating level of
251 total (C-terminal) FGF23 increased over 30-fold, while intact FGF23 increased around
252 10-fold, in both control and *Furin*^{osb}*-/-* mice (Figure 3K-L). Following the IL-1β treatment
253 the ratio of intact over C-terminal FGF23 level decreased from 60% to less than 10% in
254 both control and mutant mice (Figure 3M) and the plasma concentration of cleaved
255 FGF23 increased more than 10 times (Figure 3N). Together, these data show that
256 FGF23 processing occurs normally following rhEPO or IL-1β injections in the absence
257 of furin in osteoblasts and osteocytes,
258

259 **Normal FGF23 processing in mice lacking furin in osteoblasts, osteocytes and**
260 **hematopoietic cells following rhEPO injections**

261 The data presented above suggest that FGF23 was normally processed following
262 rhEPO or IL-1β injection in *Furin*^{osb}*-/-* mice. Osteoblasts and osteocytes are the main
263 source of circulating FGF23 in normal conditions [27,28], but bone marrow hematopoietic
264 cells contribute to approximately 40% of circulating FGF23 following rhEPO treatment
265 [27]. Therefore, in *Furin*^{osb}*-/-* mice, bone marrow hematopoietic cells could still be a
266 significant source of cleaved FGF23 following rhEPO injections. To test this possibility,
267 we generated mice lacking furin in all bone marrow hematopoietic cells (*Furin*^{BM}*-/-*) by
268 breeding *Furin*$^{flox/flox}$ mice with *Vav1-Cre*. *Vav1-Cre* transgenic animals expresses the
269 Cre recombinase under the control of the *Vav1* promoter, allowing the efficient deletion
270 of furin in fetal and adult hematopoietic stem cells (HSC) [29] and hence in all
271 hematopoietic cells. To address any potential redundancy between osteocytes and

272 hematopoietic cells in the cleavage of FGF23, we also generated mice lacking *Furin* in
273 both cell types, i.e., *Furin*$^{flox/flox}$;hOCN-Cre;Vav1-Cre mice (*Furin*$^{osb;BM}$*-/-*). Furin
274 deficiency in T cells impairs the function of regulatory and effector T cells, causing at
275 around 6 month of age severe inflammatory bowel disease, weight loss, ruffled hair and
276 hunched appearance [30]. Confirming efficient inactivation of *Furin* in hematopoietic cells,
277 these defects were also observed in our *Furin*^{BM}*-/-* mice between 4 and 6 months of age
278 (data not shown). Hence, in the following experiments all mice were 8 weeks of age, an
279 age when *Furin*^{BM}*-/-* mice are still healthy.

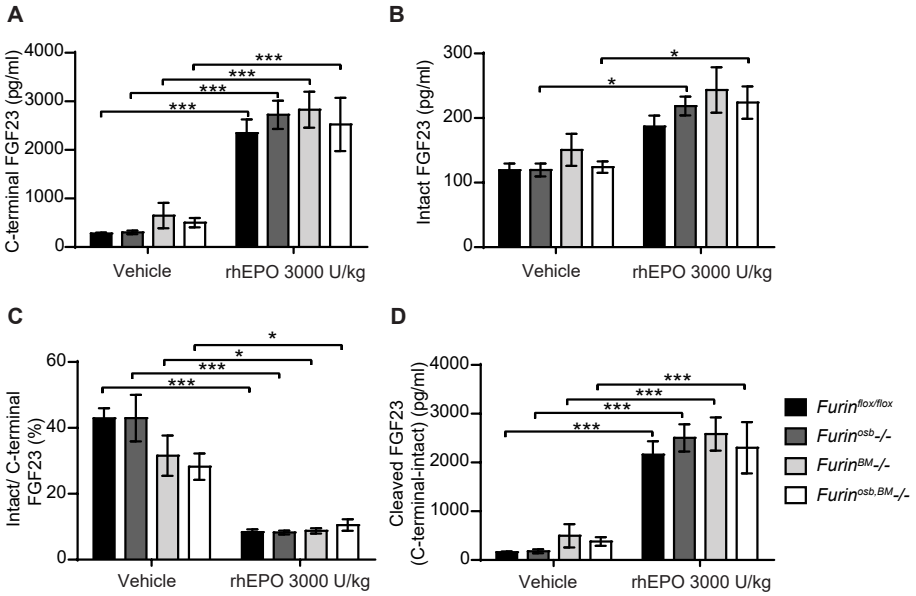

280 **Figure 4: *Furin* inactivation in osteoblasts, osteocytes and hematopoietic cells did not impair**
281 **FGF23 processing following erythropoietin injection.** Plasma FGF23 measurements in 8-week-old
282 *Furin*$^{flox/flox}$ (n=7), *Furin*^{osb}*-/-* (n=5), *Furin*^{osb}*-/-* (n=5) and *Furin*$^{osb;BM}$*-/-* (n=6) mice 6 hours following injection
283 of vehicle or 3000 U/kg of recombinant human erythropoietin (rhEPO): C-terminal FGF23 **(A)**, intact
284 FGF23 **(B)**, percentage (%) of intact over C-terminal FGF23 **(C)** and cleaved FGF23 levels **(D)**, calculated
285 as (C-terminal FGF23) - (intact FGF23). Results represent the mean ± SEM. *$P < 0.05$ and ***$P < 0.001$,
286 by 2-way ANOVA with Bonferroni's multiple comparisons test.
287

288 A single injection of rhEPO (3000U/kg) increased circulating total (C-terminal) FGF23 by
289 20-30 fold and intact FGF23 by about 2 fold in *Furin*$^{flox/flox}$, *Furin*^{osb}*-/-*, *Furin*^{BM}*-/-* and
290 *Furin*$^{osb;BM}$*-/-* mice (Figure 4A-B). The same treatment also reduced the ratio of intact

291 over C-terminal FGF23 from 40% to <10%, while plasma cleaved FGF23 level
292 increased to the same extent (>10 fold) in mice of all genotypes (Figure 4C-D).
293 Together these results indicate that in vivo, FGF23 is still processed in absence of furin
294 in osteoblasts/osteocytes and bone marrow hematopoietic cells in physiological
295 condition and following rhEPO injections.

296
297 **Figure 5: Multiple proprotein**
298 **convertases can process FGF23**
299 **in mammalian cells. (A)** Western
300 blot analysis of the secretion media
301 (SM) from CHO-K1 cells transfected
302 with V5 tagged human FGF23
303 (hFGF23-V5) and cultured in the
304 absence (-) or presence (+) of PC
305 inhibitors, decanoyl-RVKR-CMK
306 (RVKR) (50 μM) or hexa-D-arginine
307 (D6R) (20 μM). **(B)** Western blot
308 analysis of the secretion media
309 (SM) from CHO furin-deficient FD11
310 cells co-transfected with V5 tagged
311 human FGF23 (hFGF23-V5) and
312 proprotein convertase Furin, PC5A,
313 PC5B, PACE4 or PC7. Intact and
314 processed C-terminal (CT) FGF23
315 forms are detected with V5
316 antibody.
317

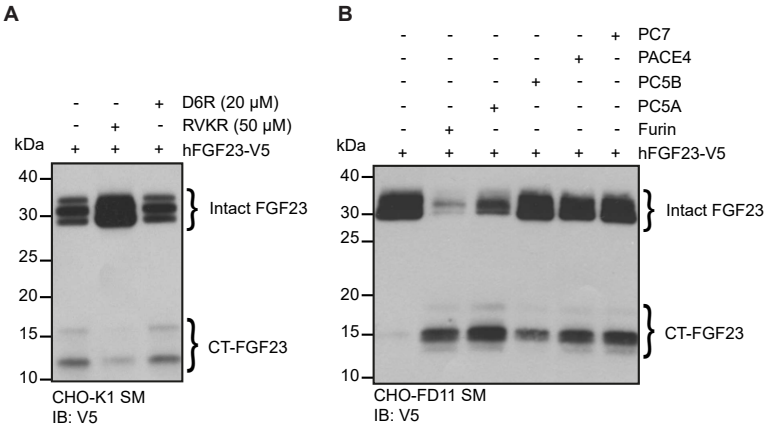

318 **Several PCs can process FGF23 in cell culture**

319 Our data suggests that in some conditions (e.g., low phosphate diet, rhEPO injection or
320 IL-1β injection), more than one PC may cleave FGF23 in vivo. In order to identify
321 additional PC(s) that might process FGF23 in vivo, we tested FGF23 processing in cell
322 lines expressing or not furin. In Chinese hamster ovary (CHO-K1) cells, which
323 endogenously express furin [31], ectopically transfected human FGF23 is secreted and
324 partially processed (Figure 5A). In the same cells, cleavage of FGF23 was inhibited by
325 decanoyl-RVKR-CMK (RVKR) a pan-PC cell-permeable inhibitor, but not by hexa-D-
326 arginine (D6R), a cell-surface PC inhibitor (Figure 5A). These observations suggest that

327 cleavage of FGF23 occurs before it is secreted, in an intracellular secretory
328 compartment, likely the trans-Golgi network [32] where furin, but also PC5A, PACE4 and
329 PC7 are present. In addition, FGF23 was not cleaved in CHO-FD11 cells, which do not
330 endogenously express furin [31], and co-transfection with a furin expressing vector was
331 sufficient to restore efficient cleavage (Figure 5B, first two lanes). We next tested the
332 capacity of other PCs, i.e., PC5A, PC5B, PACE4 and PC7 [33], to process FGF23 in
333 absence of furin in the same cells. Among all these PCs, PC5A was the most efficient in
334 processing FGF23 although PC5B, PACE4 and PC7 were also able to process FGF23
335 albeit less efficiently than PC5A (Figure 5B). Altogether, these results indicate that in
336 addition to furin, several other PCs have the capacity to process FGF23 in vitro.
337

338 **Genetic ablation of PC5 and furin in osteoblasts and osteocytes does not impair**
339 **FGF23 processing**

340 Since PC5A and PC5B, which are both encoded by *Pcsk5* [33], can cleave FGF23 in cell
341 culture, and PC5A is expressed in differentiated osteoblasts and in osteocytes [20,22], we
342 generated mice in which *Pcsk5* was inactivated specifically in osteoblasts and
343 osteocytes by breeding *Pcsk5*$^{fl/fl}$ mice [34] with hOCN-Cre transgenic animals. When fed a
344 normal chow diet, control (*Pcsk5*$^{fl/fl}$) and *Pcsk5*^{osb}*-/-* mice displayed similar circulating
345 level of intact FGF23 and serum phosphate (Figure 6A-B). Von Kossa/van Gieson
346 staining on non-decalcified bone sections did not reveal any sign of osteomalacia in
347 these mice (Figure 6C). These analyses suggest that PC5 in the osteoblast lineage is
348 dispensable for the regulation of FGF23 and phosphate levels *in vivo*.
349

350 To test if PC5 and furin redundantly cleave FGF23 *in vivo*, we next generated mice
351 lacking both furin and PC5 specifically in osteoblasts and osteocytes (i.e., *Furin*$^{flox/flox}$*;*
352 *Pcsk5*$^{flox/flox}$*;* hOCN-Cre or *Furin;Pcsk5*^{osb}*-/-* mice). Similar to the single inactivation of
353 furin in the same cells, osteoblast and osteocytes-specific inactivation of furin and PC5

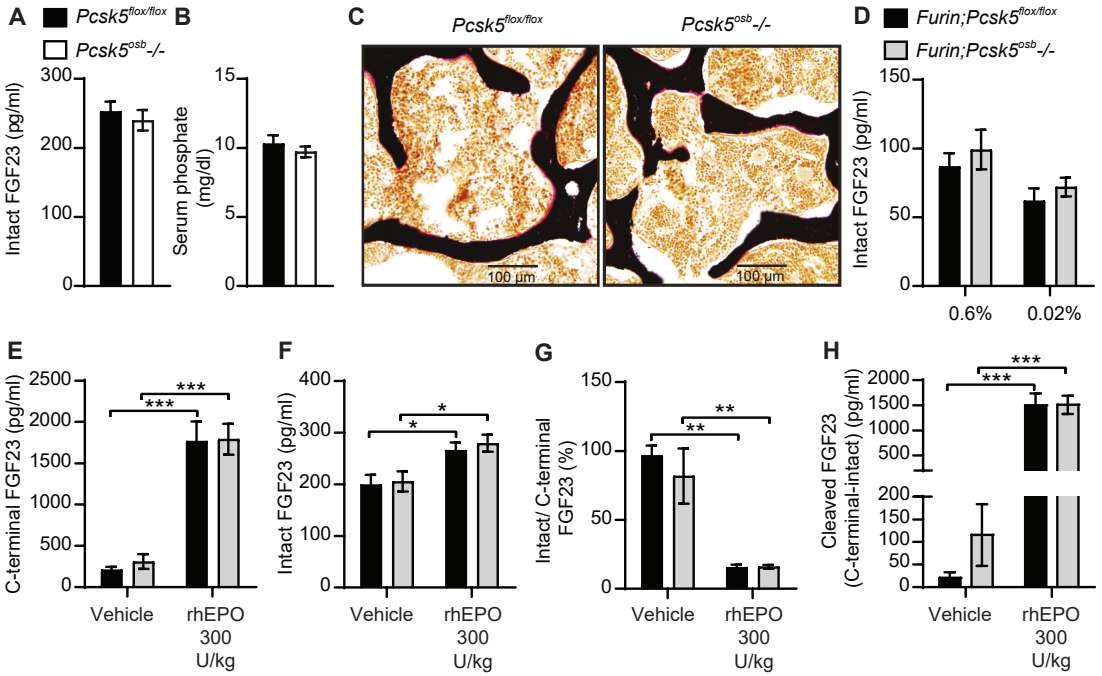

354 **Figure 6: Genetic ablation of PC5 alone or in combination with Furin does not impair FGF23**
355 **processing *in vivo*.** Plasma intact FGF23 **(A)** and serum phosphate levels **(B)** in 4-month-old *Pcsk5*$^{flox/flox}$
356 (n=6) and *Pcsk5*^{osb}*-/-* (n=7) mice fed a normal chow diet. **(C)** Von Kossa / van Gieson staining of
357 vertebrae sections of *Pcsk5*$^{flox/flox}$ and *Pcsk5*^{osb}*-/-*. **(D)** Plasma intact FGF23 in 6-month-old
358 *Furin;Pcsk5*$^{flox/flox}$ (n=7-8) and *Furin;Pcsk5*^{osb}*-/-* (n=8) fed a normal phosphate diet (0.6%) or a low
359 phosphate diet (0.02%) for one week. **(E and H)** Plasma FGF23 measurements in 4-month-old
360 *Furin;Pcsk5*$^{flox/flox}$ (n=4) and *Furin;Pcsk5*^{osb}*-/-* (n=4) 6 hours following an injection of vehicle and 300 U/kg
361 of recombinant human erythropoietin (rhEPO): C-terminal FGF23 **(E)**, intact FGF23 **(F)**, percentage (%) of
362 intact over C-terminal FGF23 **(G)** and cleaved FGF23 levels **(H)**, calculated as (C-terminal FGF23) -
363 (intact FGF23). Results represent the mean ± SEM. *$P < 0.05$ and ***$P < 0.001$, by 2-way ANOVA with
364 Bonferroni's multiple comparisons test, or by Student's t-test **(A and B)**.
365

366 resulted in a modest increase in circulating intact FGF23 levels whether mice were fed
367 normal or low phosphate diet (Figure 6D). Likewise, injection of rhEPO (300U/kg)
368 increased circulating total (C-terminal) FGF23 by almost 10-fold and intact FGF23 by
369 25% in both control and *Furin;Pcsk5*^{osb}*-/-* mice (Figure 6E-F). In these conditions,

370 plasma intact over C-terminal ratio decreased by approximately 80%, while plasma
371 cleaved FGF23 increased more than 10-fold, regardless of the mice genotype (Figure
372 6G-H). Altogether, these results show that FGF23 is still efficiently processed *in vivo*
373 even when both furin and PC5 were inactivated in osteoblasts and osteocytes.

374

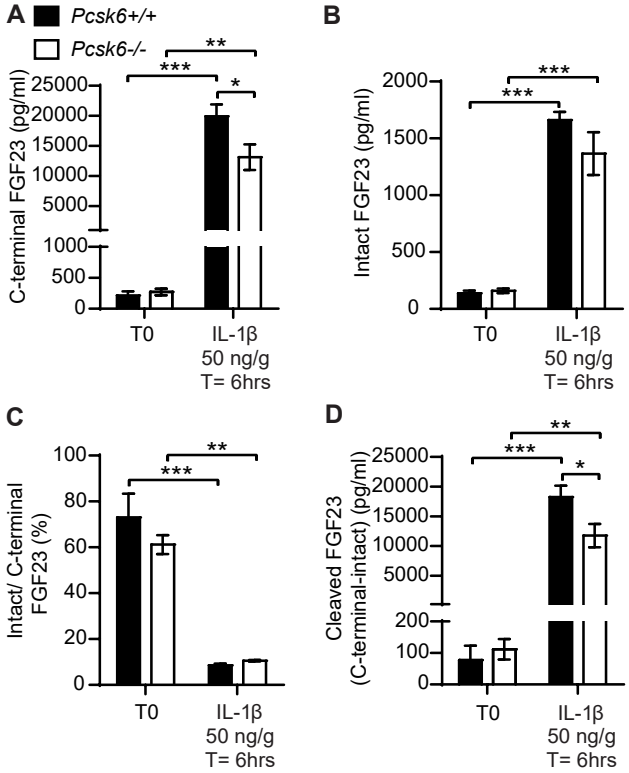

375 **Figure 7: PACE4 inactivation in mice does**
376 **not impair FGF23 processing.** Plasma
377 FGF23 measurements in 4-month-old *Pcsk6*
378 *+/+* (n=4) and *Pcsk6 -/-* (n=4) male mice before
379 (T0) and 6 hours following the injection of 50
380 ng/g of IL-1β: C-terminal FGF23 **(A)**, intact
381 FGF23 **(B)**, percentage (%) of intact over C-
382 terminal FGF23 **(C)**, and cleaved FGF23 levels
383 **(D)**, calculated as (C-terminal FGF23) - (intact
384 FGF23). Results represent the mean ± SEM.
385 **P* < 0.05 and ****P* < 0.001, by 2-way ANOVA
386 with Bonferroni's multiple comparisons test.

387

388

389

390

391

392

393 **Whole body PACE4 deletion does not impair FGF23 processing under**
394 **physiological conditions or following IL-1β injections**

395 In view of these negative results, we therefore asked whether PACE4 that is strongly
396 expressed in mouse osteoblasts [22] and can cleave FGF23 *in vitro* (Figure 5B) does so
397 in vivo. When fed a standard chow diet, *Pcsk6-/-* mice showed circulating levels of total
398 (C-terminal) and intact FGF23 that were comparable to those of wild type littermates.
399 Following a single IL-1β (50ng/g) injection, *Pcsk6-/-* mice displayed a significant

400 decrease in circulating total (C-terminal) FGF23 while intact FGF23 was not significantly
401 changed (Figure 7A and 7B). The ratio of intact over C-terminal FGF23 was equally
402 decreased after IL-1β treatment in wild type and *Pcsk6-/-* mice plasma (Figure 7C).
403 Circulating processed FGF23 was robustly increased by the same treatment regardless
404 of the genotype, although PACE4 deficient mice did displayed a significant 30%
405 reduction compared to wild type mice (Figure 7D). Altogether, these results show that
406 PACE4 may partially contribute to FGF23 expression or secretion *in vivo* in response to
407 IL-1β. Yet, FGF23 is still processed in absence of PACE4, suggesting the redundant
408 action of other PCs.
409

410 **DISCUSSION**

411

412 Over 20 years ago, mutations in a putative proprotein convertase (PC) target sequence
413 within human FGF23 were found to cause ADHR in humans. Yet, despite the critical
414 importance of this question for our understanding of phosphate metabolism, the identity
415 of the specific PC(s) involved in FGF23 cleavage *in vivo* has remained elusive. We
416 provide evidence here suggesting that furin, but not PC5, partially regulates FGF23
417 processing *in vivo* under normal conditions although this processing is by no means
418 complete. The requirement of furin for FGF23 processing appears to be context or cell-
419 type dependent, since FGF23 is still properly cleaved following rhEPO or IL-1β injection
420 when furin is inactivated alone or in combination with PC5. Our results therefore
421 suggest that additional yet to be characterized peptidases cleave FGF23 *in vivo*.

422

423 In mice fed standard chow diet, the modest increase in circulating intact FGF23
424 observed in *Furin*^{osb}*-/-* mice did not cause hypophosphatemia and osteomalacia. This
425 result is consistent with the observation that ADHR patients show variable age of onset
426 and penetrance of the disease [35]. Since iron deficiency positively correlates with intact
427 FGF23 circulating levels in ADHR patient and results in hypophosphatemia and
428 osteomalacia in mice carrying an AHDR mutation [14,15], we induced iron deficiency in
429 control and furin deficient mice. Even under these conditions, furin deficient mice did not
430 develop hypophosphatemia and in fact displayed higher serum phosphate level despite
431 a near complete impairment of FGF23 cleavage. These observations suggest that
432 although furin may be important for the cleavage of FGF23 in osteocytes in the context

433 of iron deficiency, it may also be involved in the regulation of phosphate metabolism
434 through FGF23-independent mechanism(s).
435
436 The results obtained in the context of iron deficiency raised the question as to whether,
437 under normal conditions, FGF23 may also be cleaved by another PC that would be
438 downregulated in osteocytes following iron deficiency. To clarify whether FGF23
439 cleavage by furin is context specific, we injected controls and furin-deficient mice with
440 rhEPO or IL-1β. These two circulating factors are produced in response to anemia and
441 inflammation respectively [16,36], and induce cleaved FGF23 secretion in bone and bone
442 marrow cells in rodents [16-19,26,27]. Herein, despite a strong increase in circulating total
443 (C-terminal) FGF23 level following rhEPO or IL-1β injection, *Furin*^{osb}*-/-* mice did not
444 show a concurrent increase in intact FGF23 suggesting that either cleavage of FGF23
445 occurs by one or several other PC(s) in osteocytes, or that cleaved FGF23 originates
446 mainly from bone marrow hematopoietic cells in this context. To address this second
447 possibility, we generated mice deficient in furin in osteoblast-derived cells and/or in all
448 hematopoietic cells. Our data shows that in these two cellular compartments, furin is
449 dispensable for FGF23 cleavage following the injection of rhEPO further supporting the
450 notion that furin is not the only peptidase involved in FGF23 processing *in vivo*.
451
452 PC5 (*Pcsk5*), PACE4 (*Pcsk6*) and PC7 (*Pcsk7*) are expressed in differentiated
453 osteoblasts [22] and these PCs also target the minimal consensus cleavage site (i.e.,
454 RXXR) recognized by furin [37], suggesting that these enzymes may also cleave FGF23.
455 Despite that, inactivation of *Pcsk5* specifically in osteoblasts and osteocytes did not

456 impact intact FGF23 level and serum phosphate concentrations. In addition, mice
457 deficient in both furin and PC5 in the osteoblast lineage are comparable to control mice
458 in terms of FGF23 circulating level under physiological conditions and following rhEPO
459 injection, suggesting that PC5 does not compensate for furin absence *in vivo*. Finally,
460 even though PACE4 is highly expressed in differentiated osteoblasts [22] and cleaves
461 FGF23 in mammalian cells, *Pcsk6* inactivation in mice only reduced FGF23 production
462 following IL-1β injection and did not impact its cleavage.
463
464 Altogether, these findings provide genetic evidence that furin in osteoblasts and
465 osteocytes is only partially responsible for FGF23 processing *in vivo*. Our data also
466 showed that FGF23 cleavage is differentially regulated depending on the physiological
467 context. Under conditions of iron deficiency furin is responsible for this process, while
468 following single injection of rhEPO or IL-1β, additional proteases may be involved in
469 FGF23 processing. Alternately, the increase in cleaved FGF23 following rhEPO and IL-
470 1β injection could originate from non-osteoblastic cells such as bone marrow
471 hematopoietic cells and involve multiple proteases including or not furin. Our study also
472 excluded PC5 and PACE4 as major FGF23 processing enzymes *in vivo.* In conclusion,
473 additional studies are required to determine precisely which enzyme(s) are involved in
474 FGF23 cleavage *in vivo* and how furin regulates phosphate metabolism independently
475 of FGF23.

476 **MATERIALS AND METHODS**

477

478 ***Mice and diets***

479 *Furin*$^{flox/flox}$ and *Pcsk5*$^{flox/flox}$ mice were generated by introducing loxP site flanking exon 2
480 of furin gene and exon 1 of Pcsk5 gene as described previously [38,39]. To generate
481 conditional knockout of furin (*Furin*^{osb}*-/-*) or PC5 (*Pcsk5*^{osb}*-/-*) in osteoblasts and
482 osteocytes, *Furin*$^{flox/flox}$ and *Pcsk5*$^{flox/flox}$ were crossed with OCN-Cre transgenic mice [22],
483 which express the Cre-recombinase under the control of human osteocalcin promoter
484 [21]. *Furin;Pcsk5*^{osb}*-/-* mice are deficient in both *Furin* and *Pcsk5* in osteoblasts/osteocytes
485 and were generated by breeding *Furin*^{osb}*-/-* and *Pcsk5*$^{flox/flox}$ mice. *Furin*^{BM}*-/-* and
486 *Furin*$^{osb;BM}$*-/-* mice were generated by breeding *Furin*^{osb}*-/-* mice with *Furin*$^{flox/+}$*;Vav-iCre*
487 mice. The Vav-iCre expresses the Cre recombinase under the control of the *Vav*
488 promoter, allowing the efficient deletion of furin in fetal and adult hematopoietic stem
489 cells (HSC) [29]. *Pcsk6-/-* mice were provided by Dr. Robert Day (Université de
490 Sherbrooke), these mice were generated as described previously [40]. All mice were
491 backcrossed at least 10 time with the C57BL/6J genetic background, they were
492 maintained at the IRCM pathogen free animal facility on 12h light/dark cycle and fed a
493 normal chow diet. In all experiments, unless otherwise indicated, female mice were
494 used.

495

496 In some indicated experiments mice were fed synthetic diet to induce iron or phosphate
497 deficiency. To induce iron deficiency, after weaning at 21 days old, mice were fed either
498 with normal chow diet or an iron deficient diet (Research diet, AIN-76A modified rodent

499 diet, D09070102i) for 14 weeks in combination with bleeding equivalent to one blood
500 capillary (70 μl) every two weeks. To induce phosphate deficiency, mice were fed for 5
501 days a normal phosphate diet (Envigo custom diet TD. 98243, 0.6% phosphorus), then
502 divided to two groups. The first group was maintained for one more week on 0.6% PI
503 diet while the second group was fed a phosphate deficient diet (Envigo custom diet, TD.
504 86128, 0.02% phosphorus). In other experiments, mice fed a normal chow diet were
505 injected with vehicle (saline or PBS), 300U/kg or 3000U/kg of recombinant human
506 erythropoietin (EPREX, Janssen-Cilag) or 50ng/g IL-1β (STEMCELL Technologies). All
507 animal use complied with the guidelines of the Canadian Committee for Animal
508 Protection and was approved by IRCM Animal Care Committee.
509
510 ***Serum biochemistry***
511 Intact and C-terminal FGF23 measurements were performed on EDTA plasma collected
512 from mice under fed conditions using ELISA assay specific for mouse intact or C-
513 terminal FGF23 (Quidel, cat#: 60-6800 and cat#: 60-6300). Since C-terminal FGF23
514 ELISA detects both intact and processed FGF23, it reflects the total concentration of
515 FGF23 in the circulation. We also calculated the level of cleaved FGF23 by subtracting
516 intact from C-terminal values. At end of experiments, mice were anesthetized, and
517 serum was collected by heart puncture. Serum phosphate level was determined using a
518 phosphorus assay kit (Sekisui Diagnostic, cat#:117-30). For urine phosphate
519 measurements, urine was collected in the morning for 3 consecutive days and
520 phosphate level was normalized to creatinine measured using creatinine assay (Quidel,
521 cat#: 8009).

522

523 ***RNA extraction***

524 Liver, kidney and bone marrow RNA was extracted using the standard protocol
525 previously described by Chomczynski *et al* [41], while bone RNA was extracted using
526 Trizol reagent (Thermo Fisher). cDNA was generated by RNA reverse transcription
527 using M-MLV Reverse Transcriptase (Thermo Fisher). Quantitative real-time PCR
528 (qPCR) was performed using specific primers (Key Resources Table Appendix) and
529 SYBR Green qPCR Master Mix (BiMake). Expression levels were normalized to *Actb*
530 expression levels.

531

532 ***Von Kossa/ Van Gieson staining***

533 Mouse skeletons were collected and fixed in 10% formalin for 24 hours and in 70%
534 ethanol for at least an additional 24 hours. Lumbar vertebrae were collected and
535 dehydrated by gradual increase of ethanol percentage. Vertebrae were then embedded
536 in methyl methacrylate resin as described previously [42]. Vertebrae were sectioned at 7-
537 µm sections and stained with Von kossa/Van Gieson and images were analyzed using
538 the Osteomeasure analysis system (Osteometrics, Atlanta, GA).

539

540 ***FGF23 processing in cell culture***

541 The cDNAs coding for human furin, PC7, and PACE4, and mouse PC5A and PC5B
542 were cloned into the pIRES2-EGFP vector [43], while the cDNA of hFGF23 was cloned in
543 pIRES2-EGFP-V5. CHO-K1 and furin-deficient CHO-FD11 cells were cultured at 37 °C
544 and 5% CO_2 in Ham's F-12 medium supplemented with 10% (v/v) FBS [44] and

545 transfected with 3 μg of plasmid following the standard protocol for Lipofectamine 2000
546 (Thermo Fisher). For the PCs inhibition, CHO-K1 cells were transfected with cDNAs
547 encoding for hFGF23-V5 and PCs in the ratio of 5:1 and 24 hours later pretreated for 5
548 hours with Dec-RVKR-CMK (50 μM; Tocris) or D6R (20 μM; Calbiochem) followed by 22
549 hours of treatment in serum free media. Cells supernatant was then collected in the
550 presence of 1x complete protease inhibitor cocktail (Roche) and FGF23 processing was
551 analyzed by SDS-PAGE (15% Tris-glycine) followed by western blot using V5 antibody
552 (Thermo Fisher).
553
554 ***Statistics***
555 Statistical analyses were performed using GraphPad Prism software version 7.03.
556 Results are shown as the mean ± SEM. Unpaired, 2-tailed Student's *t* test was used for
557 single measurements or comparison between two groups, while 1-way or 2-way
558 ANOVA followed by Bonferroni's post-test were used for comparison of more than 2
559 groups. A *P* value of less than 0.05 was considered statistically significant. All
560 experiments were performed at least on 3 independent animals. Before starting each *in*
561 *vivo* experiment, the mice were randomized into experimental groups with similar
562 average body weight.
563
564

565 **ACKNOWLEDGEMENTS**

566 We thank Dr. R. Day for providing *Pcsk6*$^{-/-}$ mice, Dr. T. Clemens for sharing the hOC-
567 Cre mice and Dr. T. Möröy for the iVav-Cre strain. This work was supported by funding
568 from the Canada Research Chair program (M.F.) and the Natural Sciences and
569 Engineering Research Council of Canada (RGPIN-2016-05213, to MF) and a CIHR
570 Foundation grant (# 148363 to NGS). OAR received scholarships from IRCM and
571 FRQS.

572

573 **CONFLICTS OF INTERESTS**

574 O.A.R., D.S.R., R.E., J.W.M.C., N.G.S., and M.F. have nothing to declare.
575

576

577 **REFERENCES**

578

579 1 Meyer, R. A., Jr., Meyer, M. H. & Gray, R. W. Parabiosis suggests a humoral
580 factor is involved in X-linked hypophosphatemia in mice. *J Bone Miner Res* **4**,
581 493-500, doi:10.1002/jbmr.5650040407 (1989).
582 2 Miyauchi, A., Fukase, M., Tsutsumi, M. & Fujita, T. Hemangiopericytoma-induced
583 osteomalacia: tumor transplantation in nude mice causes hypophosphatemia and
584 tumor extracts inhibit renal 25-hydroxyvitamin D 1-hydroxylase activity. *J Clin*
585 *Endocrinol Metab* **67**, 46-53, doi:10.1210/jcem-67-1-46 (1988).
586 3 Urakawa, I. *et al.* Klotho converts canonical FGF receptor into a specific receptor
587 for FGF23. *Nature* **444**, 770-774, doi:10.1038/nature05315 (2006).
588 4 Larsson, T. *et al.* Transgenic mice expressing fibroblast growth factor 23 under
589 the control of the alpha1(I) collagen promoter exhibit growth retardation,
590 osteomalacia, and disturbed phosphate homeostasis. *Endocrinology* **145**, 3087-
591 3094, doi:10.1210/en.2003-1768 (2004).
592 5 Shimada, T. *et al.* FGF-23 is a potent regulator of vitamin D metabolism and
593 phosphate homeostasis. *J Bone Miner Res* **19**, 429-435,
594 doi:10.1359/JBMR.0301264 (2004).
595 6 Shimada, T. *et al.* Targeted ablation of Fgf23 demonstrates an essential
596 physiological role of FGF23 in phosphate and vitamin D metabolism. *J Clin Invest*
597 **113**, 561-568, doi:10.1172/JCI19081 (2004).
598 7 Shimada, T. *et al.* FGF-23 transgenic mice demonstrate hypophosphatemic
599 rickets with reduced expression of sodium phosphate cotransporter type IIa.
600 *Biochem Biophys Res Commun* **314**, 409-414, doi:10.1016/j.bbrc.2003.12.102
601 (2004).
602 8 Benet-Pages, A., Orlik, P., Strom, T. M. & Lorenz-Depiereux, B. An FGF23
603 missense mutation causes familial tumoral calcinosis with hyperphosphatemia.
604 *Hum Mol Genet* **14**, 385-390, doi:10.1093/hmg/ddi034 (2005).
605 9 Ichikawa, S. *et al.* Genetic rescue of glycosylation-deficient Fgf23 in the Galnt3
606 knockout mouse. *Endocrinology* **155**, 3891-3898, doi:10.1210/en.2014-1199
607 (2014).
608 10 Topaz, O. *et al.* Mutations in GALNT3, encoding a protein involved in O-linked
609 glycosylation, cause familial tumoral calcinosis. *Nat Genet* **36**, 579-581,
610 doi:10.1038/ng1358 (2004).
611 11 Tagliabracci, V. S. *et al.* Dynamic regulation of FGF23 by Fam20C
612 phosphorylation, GalNAc-T3 glycosylation, and furin proteolysis. *Proc Natl Acad*
613 *Sci U S A* **111**, 5520-5525, doi:10.1073/pnas.1402218111 (2014).
614 12 Consortium, A. Autosomal dominant hypophosphataemic rickets is associated
615 with mutations in FGF23. *Nat Genet* **26**, 345-348, doi:10.1038/81664 (2000).
616 13 Nesbitt, T., Coffman, T. M., Griffiths, R. & Drezner, M. K. Crosstransplantation of
617 kidneys in normal and Hyp mice. Evidence that the Hyp mouse phenotype is
618 unrelated to an intrinsic renal defect. *J Clin Invest* **89**, 1453-1459,
619 doi:10.1172/JCI115735 (1992).
620 14 Imel, E. A. *et al.* Iron modifies plasma FGF23 differently in autosomal dominant
621 hypophosphatemic rickets and healthy humans. *J Clin Endocrinol Metab* **96**,
622 3541-3549, doi:10.1210/jc.2011-1239 (2011).

15 Farrow, E. G. *et al.* Iron deficiency drives an autosomal dominant hypophosphatemic rickets (ADHR) phenotype in fibroblast growth factor-23 (Fgf23) knock-in mice. *Proc Natl Acad Sci U S A* **108**, E1146-1155, doi:10.1073/pnas.1110905108 (2011).

16 David, V. *et al.* Inflammation and functional iron deficiency regulate fibroblast growth factor 23 production. *Kidney Int* **89**, 135-146, doi:10.1038/ki.2015.290 (2016).

17 Hanudel, M. R. *et al.* Effects of erythropoietin on fibroblast growth factor 23 in mice and humans. *Nephrol Dial Transplant*, doi:10.1093/ndt/gfy189 (2018).

18 Flamme, I., Ellinghaus, P., Urrego, D. & Kruger, T. FGF23 expression in rodents is directly induced via erythropoietin after inhibition of hypoxia inducible factor proline hydroxylase. *PLoS One* **12**, e0186979, doi:10.1371/journal.pone.0186979 (2017).

19 Daryadel, A. *et al.* Erythropoietin stimulates fibroblast growth factor 23 (FGF23) in mice and men. *Pflugers Arch* **470**, 1569-1582, doi:10.1007/s00424-018-2171-7 (2018).

20 Yamamoto, H. *et al.* Posttranslational processing of FGF23 in osteocytes during the osteoblast to osteocyte transition. *Bone* **84**, 120-130, doi:10.1016/j.bone.2015.12.055 (2016).

21 Zhang, M. *et al.* Osteoblast-specific knockout of the insulin-like growth factor (IGF) receptor gene reveals an essential role of IGF signaling in bone matrix mineralization. *J Biol Chem* **277**, 44005-44012 (2002).

22 Al Rifai, O. *et al.* Proprotein convertase furin regulates osteocalcin and bone endocrine function. *J Clin Invest* **127**, 4104-4117, doi:10.1172/JCI93437 (2017).

23 Bon, N. *et al.* Phosphate-dependent FGF23 secretion is modulated by PiT2/Slc20a2. *Mol Metab* **11**, 197-204, doi:10.1016/j.molmet.2018.02.007 (2018).

24 Yu, X., Sabbagh, Y., Davis, S. I., Demay, M. B. & White, K. E. Genetic dissection of phosphate- and vitamin D-mediated regulation of circulating Fgf23 concentrations. *Bone* **36**, 971-977, doi:10.1016/j.bone.2005.03.002 (2005).

25 Perwad, F. *et al.* Dietary and serum phosphorus regulate fibroblast growth factor 23 expression and 1,25-dihydroxyvitamin D metabolism in mice. *Endocrinology* **146**, 5358-5364, doi:10.1210/en.2005-0777 (2005).

26 Toro, L. *et al.* Erythropoietin induces bone marrow and plasma fibroblast growth factor 23 during acute kidney injury. *Kidney Int* **93**, 1131-1141, doi:10.1016/j.kint.2017.11.018 (2018).

27 Clinkenbeard, E. L. *et al.* Erythropoietin stimulates murine and human fibroblast growth factor-23, revealing novel roles for bone and bone marrow. *Haematologica* **102**, e427-e430, doi:10.3324/haematol.2017.167882 (2017).

28 Clinkenbeard, E. L. *et al.* Conditional Deletion of Murine Fgf23: Interruption of the Normal Skeletal Responses to Phosphate Challenge and Rescue of Genetic Hypophosphatemia. *J Bone Miner Res* **31**, 1247-1257, doi:10.1002/jbmr.2792 (2016).

29 de Boer, J. *et al.* Transgenic mice with hematopoietic and lymphoid specific expression of Cre. *European journal of immunology* **33**, 314-325, doi:10.1002/immu.200310005 (2003).

30 Pesu, M. *et al.* T-cell-expressed proprotein convertase furin is essential for maintenance of peripheral immune tolerance. *Nature* **455**, 246-250 (2008).

31 Susan-Resiga, D. *et al.* Furin is the major processing enzyme of the cardiac-specific growth factor bone morphogenetic protein 10. *J Biol Chem* **286**, 22785-22794, doi:10.1074/jbc.M111.233577 (2011).

32 Susan-Resiga, D. *et al.* Furin Is the Major Processing Enzyme of the Cardiac-specific Growth Factor Bone Morphogenetic Protein 10. *J Biol. Chem.* **286**, 22785-22794 (2011).

33 Seidah, N. G. & Prat, A. The biology and therapeutic targeting of the proprotein convertases. *Nat Rev Drug Discov.* **11**, 367-383 (2012).

34 Essalmani, R. *et al.* In vivo functions of the proprotein convertase PC5/6 during mouse development: Gdf11 is a likely substrate. *Proc. Natl. Acad. Sci. U. S. A.* **105**, 5750-5755 (2008).

35 Imel, E. A., Hui, S. L. & Econs, M. J. FGF23 concentrations vary with disease status in autosomal dominant hypophosphatemic rickets. *J Bone Miner Res* **22**, 520-526, doi:10.1359/jbmr.070107 (2007).

36 Jelkmann, W. Regulation of erythropoietin production. *J Physiol* **589**, 1251-1258, doi:10.1113/jphysiol.2010.195057 (2011).

37 Seidah, N. G. & Prat, A. The biology and therapeutic targeting of the proprotein convertases. *Nature reviews. Drug discovery* **11**, 367-383 (2012).

38 Essalmani, R. *et al.* In vivo functions of the proprotein convertase PC5/6 during mouse development: Gdf11 is a likely substrate. *Proceedings of the National Academy of Sciences of the United States of America* **105**, 5750-5755, doi:10.1073/pnas.0709428105 (2008).

39 Roebroek, A. J. *et al.* Limited redundancy of the proprotein convertase furin in mouse liver. *J Biol Chem* **279**, 53442-53450, doi:10.1074/jbc.M407152200 (2004).

40 Constam, D. B. & Robertson, E. J. SPC4/PACE4 regulates a TGFbeta signaling network during axis formation. *Genes & development* **14**, 1146-1155 (2000).

41 Chomczynski, P. & Sacchi, N. The single-step method of RNA isolation by acid guanidinium thiocyanate-phenol-chloroform extraction: twenty-something years on. *Nature protocols* **1**, 581-585, doi:10.1038/nprot.2006.83 (2006).

42 Chappard, D., Palle, S., Alexandre, C., Vico, L. & Riffat, G. Bone embedding in pure methyl methacrylate at low temperature preserves enzyme activities. *Acta Histochem* **81**, 183-190 (1987).

43 Bergeron, E. *et al.* Implication of proprotein convertases in the processing and spread of severe acute respiratory syndrome coronavirus. *Biochem Biophys Res Commun* **326**, 554-563, doi:10.1016/j.bbrc.2004.11.063 (2005).

44 Gordon, V. M., Rehemtulla, A. & Leppla, S. H. A role for PACE4 in the proteolytic activation of anthrax toxin protective antigen. *Infection and immunity* **65**, 3370-3375, doi:10.1128/IAI.65.8.3370-3375.1997 (1997).

711 **FIGURES LEGENDS**

712

713 **Figure 1: Increased FGF23 level and reduced phosphate excretion in *Furin^{osb}-/-***
714 **mice.** FGF23 and phosphate levels in in 4-month-old *Furin$^{flox/flox}$* (n=6) and *Furin^{osb}-/-*
715 (n=6) mice fed on normal chow diet **(A-D)**. Intact FGF23 levels in plasma **(A)**. FGF23
716 target genes expression in kidney **(B)**. Serum phosphate level **(C)**. Von Kossa / van
717 Gieson staining on vertebrae sections **(D)**. FGF23 and phosphate parameters in 6-
718 months-old *Furin$^{flox/flox}$* (n=6) and *Furin^{osb}-/-* (n=6-7) mice fed a normal phosphate diet
719 (0.6%) or a low phosphate diet (0.02%) for one week **(E-N)**. Body weight **(E)**. Kidney
720 weight normalize to body weight **(F)**. Serum phosphate levels **(G)**. Plasma level of C-
721 terminal FGF23 **(H)**, intact FGF23 **(I)**, percentage (%) of intact over C-terminal FGF23
722 **(J)** and cleaved FGF23 levels **(K)** calculated as (C-terminal FGF23) - (intact FGF23).
723 Expression level in kidney of the sodium phosphate cotransporter *Slc34a1* **(L)** and
724 *Slc34a3* **(M). (N)** Urine phosphate measurements normalized to creatinine. Results
725 represent the mean ± SEM. *P < 0.05, **P < 0.01, and ***P < 0.001, by 2-way ANOVA
726 with Bonferroni's multiple comparisons test or by Student's t-test (A, C, G, H, K, and M)
727 #: P<0.05; # #: P<0.01, # # #: P<0.001 &: 0.05<P<0.1.

728

729 **Figure 2: Impaired FGF23 processing in *Furin^{osb}-/-* mice following iron restriction.**
730 *Furin$^{flox/flox}$* (n=3-5) and *Furin^{osb}-/-* (n=7-8) 21-day-old mice were fed normal chow diet
731 (ND) or a low iron diet (LI) for 14 weeks. **(A)** Body weight growth curve presented as
732 percentage of initial body weight. **(B-C)** Expression of iron-regulated genes in liver.
733 Hepcidin (*Hamp*) expression **(B)**. Transferrin receptor (*Tfrc*) expression **(C). (D)** *Fgf23*
734 expression in long bone. **(E-H**) Plasma level of C-terminal FGF23 **(E)**, intact FGF23 **(F)**,

735 percentage (%) of intact over C-terminal FGF23 **(G)** and cleaved FGF23 levels **(H)**,
736 calculated as (C-terminal FGF23) - (intact FGF23). **(I)** Serum phosphate levels. Results
737 represent the mean ± SEM. *P < 0.05, **P < 0.01, and ***P < 0.001, by 2-way ANOVA
738 with Bonferroni's multiple comparisons test or by Student's t-test (D and E) #: P<0.05; #
739 #: P<0.01, # # #: P<0.001 &: 0.05<P<0.1.
740

741 **Figure 3: FGF23 is normally processed following erythropoietin and IL-1β**
742 **injection in *Furin^{osb}-/-* mice.** Genes expression in long bone **(A, B and E)** and bone
743 marrow **(C, D and F)** of 2-month-old C57BL/6J mice 6 hours following the injection of
744 vehicle (n=4), 300 U/kg (n=4) or 3000 U/kg (n=4) of recombinant human erythropoietin
745 (rhEPO). Erythropoietin receptor (*Epor*) **(A and C)**, erythroferrone (*Erfe*) **(B and D)** and
746 FGF23 (*Fgf23*) **(C and F)**. **(G-J)** Plasma FGF23 measurements in 4-month-old
747 *Furin$^{flox/flox}$* (n=3) and *Furin^{osb}-/-* (n=3) mice 6 hours following the injection of vehicle, 300
748 U/kg or 3000 U/kg of rhEPO. C-terminal FGF23 **(G)**, intact FGF23 **(H),** percentage (%)
749 of intact over C-terminal FGF23 **(I)** and cleaved FGF23 levels **(J)**, calculated as (C-
750 terminal FGF23) - (intact FGF23). **(K-N)** Plasma FGF23 measurements in 4-month-old
751 *Furin$^{flox/flox}$* (n=4) and *Furin^{osb}-/-* (n=4) mice before (T0) and 6 hours following the
752 injection of 50 ng/g IL-1β (T=6hrs). C-terminal FGF23 **(K)**, intact FGF23 **(L),** percentage
753 (%) of intact over C-terminal FGF23 **(M)** and cleaved FGF23 levels **(N)**. Results
754 represent the mean ± SEM. *P < 0.05, **P < 0.01, and ***P < 0.001, by 1-way ANOVA
755 **(A-F)** or 2-way ANOVA **(G-N)** with Bonferroni's multiple comparisons test, or by
756 Student's t-test **(A and E)** #: P<0.05; # #: P<0.01, # # #: P<0.001 &: 0.05<P<0.1.
757

758 **Figure 4: *Furin* inactivation in osteoblasts, osteocytes and hematopoietic cells**
759 **did not impair FGF23 processing following erythropoietin injection.** Plasma FGF23
760 measurements in 8-week-old *Furin*$^{flox/flox}$ (n=7), *Furin*^{osb}*-/-* (n=5), *Furin*^{osb}*-/-* (n=5) and
761 *Furin*$^{osb;BM}$*-/-* (n=6) mice 6 hours following injection of vehicle or 3000 U/kg of
762 recombinant human erythropoietin (rhEPO): C-terminal FGF23 **(A)**, intact FGF23 **(B)**,
763 percentage (%) of intact over C-terminal FGF23 **(C)** and cleaved FGF23 levels **(D)**,
764 calculated as (C-terminal FGF23) - (intact FGF23). Results represent the mean ± SEM.
765 *P < 0.05 and ***P < 0.001, by 2-way ANOVA with Bonferroni's multiple comparisons
766 test.
767
768 **Figure 5: Multiple proprotein convertases can process FGF23 in mammalian cells.**
769 **(A)** Western blot analysis of the secretion media (SM) from CHO-K1 cells transfected
770 with V5 tagged human FGF23 (hFGF23-V5) and cultured in the absence (-) or presence
771 (+) of PC inhibitors, decanoyl-RVKR-CMK (RVKR) (50 μM) or hexa-D-arginine (D6R)
772 (20 μM). **(B)** Western blot analysis of the secretion media (SM) from CHO furin-deficient
773 FD11 cells co-transfected with V5 tagged human FGF23 (hFGF23-V5) and proprotein
774 convertase Furin, PC5A, PC5B, PACE4 or PC7. Intact and processed C-terminal (CT)
775 FGF23 forms are detected with V5 antibody.
776
777 **Figure 6: Genetic ablation of PC5 alone or in combination with Furin does not**
778 **impair FGF23 processing *in vivo*.** Plasma intact FGF23 **(A)** and serum phosphate
779 levels **(B)** in 4-month-old *Pcsk5*$^{flox/flox}$ (n=6) and *Pcsk5*^{osb}*-/-* (n=7) mice fed a normal
780 chow diet. **(C)** Von Kossa / van Gieson staining of vertebrae sections of *Pcsk5*$^{flox/flox}$ and

781 *Pcsk5*^{osb}*-/-*. **(D)** Plasma intact FGF23 in 6-month-old *Furin;Pcsk5*$^{flox/flox}$ (n=7-8) and
782 *Furin;Pcsk5*^{osb}*-/-* (n=8) fed a normal phosphate diet (0.6%) or a low phosphate diet
783 (0.02%) for one week. **(E and H)** Plasma FGF23 measurements in 4-month-old
784 *Furin;Pcsk5*$^{flox/flox}$ (n=4) and *Furin;Pcsk5*^{osb}*-/-* (n=4) 6 hours following an injection of
785 vehicle and 300 U/kg of recombinant human erythropoietin (rhEPO): C-terminal FGF23
786 **(E)**, intact FGF23 **(F)**, percentage (%) of intact over C-terminal FGF23 **(G)** and cleaved
787 FGF23 levels **(H)**, calculated as (C-terminal FGF23) - (intact FGF23). Results represent
788 the mean ± SEM. **P* < 0.05 and ****P* < 0.001, by 2-way ANOVA with Bonferroni's
789 multiple comparisons test, or by Student's t-test **(A and B)**.
790
791 **Figure 7: PACE4 inactivation in mice does not impair FGF23 processing.** Plasma
792 FGF23 measurements in 4-month-old *Pcsk6 +/+* (n=4) and *Pcsk6 -/-* (n=4) male mice
793 before (T0) and 6 hours following the injection of 50 ng/g of IL-1β: C-terminal FGF23
794 **(A)**, intact FGF23 **(B)**, percentage (%) of intact over C-terminal FGF23 **(C)**, and cleaved
795 FGF23 levels **(D)**, calculated as (C-terminal FGF23) - (intact FGF23). Results represent
796 the mean ± SEM. **P* < 0.05 and ****P* < 0.001, by 2-way ANOVA with Bonferroni's
797 multiple comparisons test.
798
799

Table Appendix: Primers used				
Reagent type (species) or resource	**Designation**	**Source or reference**	**Identifiers**	**Additional information**
Sequence-based reagent	Actin beta- For	This paper	QPCR primer (amplify *Actb*, M. musculus)	GACCTCTAT GCCAACACAGT
Sequence-based reagent	Actin beta- Rev	This paper	QPCR primer (amplify *Actb*, M. musculus)	AGTACTTGC GCTCAGGAGGA
Sequence-based reagent	Slc34a1-Fw	This paper	QPCR primer (amplify *Slc34a1*, M. musculus)	GCATCCTACTGTGGTAC CCG
Sequence-based reagent	Slc34a1-Rv	This paper	QPCR primer (amplify *Slc34a1*, M. musculus)	CAGCAAACCAGCGGTA CTTG
Sequence-based reagent	Slc34a3-Fw	This paper	QPCR primer (amplify *Slc34a3*, M. musculus)	CCTTTGGACTTTCCCTG GCA
Sequence-based reagent	Slc34a3-Rv	This paper	QPCR primer (amplify *Slc34a3*, M. musculus)	GATGGTCGGTGTTGTT GCAG
Sequence-based reagent	Hamp-Fw	This paper	QPCR primer (amplify *Hamp*, M. musculus)	AGAGCTGCAGCCTTTG CAC
Sequence-based reagent	Hamp-Rv	This paper	QPCR primer (amplify *Hamp*, M. musculus)	GAGGTCAGGATGTGGC TCTA
Sequence-based reagent	Tfrc-Fw	This paper	QPCR primer (amplify *Tfrc*, M. musculus)	TAAATTCCCCGTTGTTG AGG
Sequence-based reagent	Tfrc-Rv	This paper	QPCR primer (amplify *Tfrc*, M. musculus)	CAGGACAGCTTCCTTC CATT
Sequence-based reagent	Cyp27b1-Fw	This paper	QPCR primer (amplify *Cyp27b1*, M. musculus)	GAAGCTGCGATGAGGA ACCA
Sequence-based reagent	Cyp27b1-Rv	This paper	QPCR primer (amplify *Cyp27b1*, M. musculus)	TTCCCCACTATGGACTG GACA
Sequence-based reagent	Cyp24a1-Fw	This paper	QPCR primer (amplify *Cyp24a1*, M. musculus)	CCCAGCGGCTAGAGAT CAAA
Sequence-based reagent	Cyp24a1-Rv	This paper	QPCR primer (amplify *Cyp24a1*, M. musculus)	TTTCTTTTGGAAGGCGC TGC

Sequence-based reagent	Fgf23-Fw	This paper	QPCR primer (amplify *Fgf23*, M. musculus)	CCGCTGCTGCATTTCTACAC
Sequence-based reagent	Fgf23-Rv	This paper	QPCR primer (amplify *Fgf23*, M. musculus)	CTTGAGCACGTTCAGTGGGT
Sequence-based reagent	Epor-Fw	This paper	QPCR primer (amplify *Epor*, M. musculus)	GGACACAAAGGGTGGAGGTC
Sequence-based reagent	Epor-Rv	This paper	QPCR primer (amplify *Epor*, M. musculus)	GCTCGAACAGCGAAGGTGTA
Sequence-based reagent	Erfe-Fw	This paper	QPCR primer (amplify *Erfe*, M. musculus)	GTTCCAGCTGTTGCTGAAAGG
Sequence-based reagent	Erfe-Rv	This paper	QPCR primer (amplify *Erfe*, M. musculus)	TACCCGAGGCTGGTGTAGTG

800